New methodology for dynamic soil characterization using the free-decay response in resonant column testing

Fernando J. Tallavo, Giovanni Cascante, Mahesh D. Pandey & Sriram Narasimhan
Department of Civil and Environmental Engineering – University of Waterloo, Waterloo, Ontario, Canada

2011 Pan-Am CGS Geotechnical Conference

ABSTRACT
The resonant-column (RC) test is an ASTM standard commonly used for dynamic characterization of soils under different isotropic confinements and shear strain levels. The free-decay response of a soil specimen shows a nonlinear behaviour when the strain levels exceed the threshold shear strain. However, the dynamic parameters are commonly determined assuming a linear single-degree-of-freedom (SDOF) model. This paper presents a new analysis methodology, based on the complex exponential method (CEM), for the nonlinear dynamic characterization of soil specimens using the free-vibration response in RC testing. The effectiveness of the new methodology is demonstrated in a dry-sand specimen tested under isotropic loading and unloading conditions, two confining pressures (40 kPa and 100 kPa), and different shear-strain levels ($10^{-5} \leq \gamma_{max} \leq 1.7 \times 10^{-3}$). The results from the CEM are compared with the results from traditional SDOF methods (transfer function and free vibration). The results show that the damping ratio can be underestimated up to 80% at large strains when computed using SDOF models. In a nonlinear free-vibration test analyzed using the CEM, it is possible to observe that the dry-sand specimen becomes denser (stiffer) after large-strain cycles. Thus, the shear wave velocity (resonant frequency) increases at the low shear strain levels imposed during the same test.

RESUMEN
El ensayo de columna resonante (RC) es un estándar ASTM comúnmente usado para la caracterización dinámica de suelos sometidos a diferentes presiones de confinamiento y niveles de deformación por corte. La respuesta de vibración libre de un espécimen de suelo ensayado en RC muestra un comportamiento no-lineal cuando los niveles de deformación exceden el umbral de deformación por corte. Sin embargo, los parámetros dinámicos son comúnmente determinados asumiendo un modelo de un solo grado de libertad (SDOF). Este paper presenta una nueva metodología de análisis basada en el método exponencial complejo (CEM) para la caracterización dinámica no-lineal de especímenes de suelo usando la respuesta de vibración libre en ensayos de RC. La eficacia de la nueva metodología es demostrada en un espécimen de arena, en condición seca, ensayado bajo condiciones que carga y descarga, dos presiones de confinamiento (40 kPa y 100 kPa) y diferentes niveles de deformación por corte ($10^{-5} \leq \gamma_{max} \leq 1.7 \times 10^{-3}$). Los resultados del CEM son comparados con los valores obtenidos usando los métodos tradicionales (función de transferencia y vibración libre para un SDOF). Los resultados muestran que el factor de amortiguamiento puede ser subestimado hasta en 80 % a elevadas deformaciones por corte cuando éste es calculado usando los métodos tradicionales. Adicionalmente, la arena se hace más densa (rígida) después de la aplicación de ciclos a elevados niveles de deformación por corte. Como consecuencia, la velocidad de onda de corte (frecuencia de resonancia) aumenta a bajo niveles de deformación por corte impuestos durante la misma prueba.

1 INTRODUCTION

The resonant-column (RC) test is an ASTM standard that has been extensively used for dynamic characterization of soils under different confinement and shear strain conditions (Wilson and Dietrich 1960; Hardin and Richart 1963). In this device, a fixed-free cylindrical soil specimen is excited in torsion. The response of the specimen is measured using a piezoelectric accelerometer located at the driving plate. The shear wave velocity of the soil specimen is estimated by solving the equation of wave motion of a rod with an attached mass at the top (Hardin and Richart 1963).

The shear modulus is then determined from the shear wave velocity. The damping ratio can be obtained either from the analysis of the input excitation and the response of the specimen (frequency domain) or from the analysis in the time domain of the free-decay response when the specimen is subjected to an impulsive excitation.

The free-decay response of a soil specimen in the time domain shows a nonlinear behaviour when the strain levels exceed the threshold shear strain; however, the dynamic parameters are commonly determined assuming a linear single-degree-of-freedom (SDOF) model.

This paper presents a new analysis methodology, based on the complex exponential method (CEM, Osborne and Smyth 1995), for the nonlinear dynamic characterization of soil specimens using the free-decay response in RC testing. The nonlinear response of the soil specimen is represented as a superposition of damped exponential functions. The use of the free-decay response is also beneficial because it reduces the number of

excitation cycles imposed on the specimen during testing and thus reduces the disturbance of the specimen.

The new methodology is demonstrated on a dry-sand specimen tested under isotropic loading and unloading conditions, two confining pressures (40 kPa and 100 kPa), and different shear-strain levels ($10^{-5} \leq \gamma_{\max} \leq 1.7 \times 10^{-3}$). The results from the CEM are compared with the results from traditional linear methods (e.g. transfer function and free vibration of a SDOF system).

2 COMPLEX EXPONENTIAL METHOD (CEM)

The main advantage of the CEM with respect to Fourier analysis is the representation of transient time signals as a summation of exponential functions instead of continuous sinusoidal functions; which give a correct representation of a transient signal only when the time window tends to infinity. The CEM has two main differences with respect to the Fourier transform: a) sinusoidal functions can grow or decay; thus, damping ratios are computed directly, and b) the resolution in the frequency domain is increased because the frequencies of the exponential functions are estimated directly in the time domain.

In this work, the CEM is used for the analysis of the free-vibration response of soil specimens tested in the RC device. As a result, the dynamic properties of soil specimens are obtained (e.g. resonant frequencies, damping ratios, and maximum amplitudes of vibration corresponding to each of the damped modes).

The free vibration response of a SDOF system in discrete form is represented as

$$q_n = Ae^{-\xi\omega(n\Delta t)}\cos(\omega'(n\Delta t) + \theta) \quad [1]$$

where Δt is the interval sampling, and $n: 0, 1, \dots N_p$. For a MDOF system, Eq. 1 becomes in

$$q_n = \sum_{k=1}^{N} A_k e^{-\xi_k\omega_k(n\Delta t)} cos(\omega'_k(n\Delta t) + \theta_k) \quad [2]$$

which can also be expressed as a sum of exponential functions

$$q_n = \sum_{k=1}^{N} \tilde{A}_k {Z_k}^n \quad [3]$$

where N is the number of degrees of freedom

$$Z_k = e^{(-\xi_k\omega_k + j\omega_k')\Delta t} \quad [4]$$

and $j^2 = -1$. Taking the natural logarithm of Eq. 4, the following relationships for ω and ξ are obtained

$$\omega_k = \frac{\sqrt{(imag(\ln(Z_k)))^2 + (real(\ln(Z_k)))^2}}{\Delta t} \quad [5]$$

and

$$\xi_k = \frac{real(\ln(Z_k))}{\sqrt{(imag(\ln(Z_k)))^2 + (real(\ln(Z_k)))^2}} \quad [6]$$

The CEM is based on the evaluation of the corresponding impulse response function (IRF). Therefore, if Eq. 2 represents the IRF of a MDOF system, the transfer function is given by

$$H(Z) = \frac{B(Z)}{A(Z)} = \sum_{n=0}^{L} q_n Z^{-n} \quad [7]$$

where $B(Z)$ and $A(Z)$ are polynomial functions of orders *M* and *N* (*M* and *N* represent the number of zeros and poles, respectively). Equation 7 can be expanded as

$$b_0 + b_1Z^{-1} + \cdots b_MZ^{-M} = (y_0 + q_1Z^{-1} + \cdots q_LZ^{-L})(1 + a_1Z^{-1} + \cdots a_NZ^{-N}) \quad [8]$$

where $b_0, b_1, \dots b_M$ and $a_1, a_2, \dots a_N$ are the coefficients of the polynomials $B(Z)$ and $A(Z)$, respectively. Since these coefficients are real, the poles and zeros of $H(Z)$ occur in complex conjugate pairs. Equating powers of Z on each side Eq. 8, the following set of equations are obtained

$$\begin{aligned} b_0 &= q_0 \\ b_1 &= q_1 + q_0a_1 \\ &\cdot \\ b_M &= q_M + q_{(M-1)}a_1 + \cdots q_{(M-N)}a_N \\ 0 &= q_{(M+1)} + q_Ma_1 + \cdots q_{(M-N+1)}a_N \\ &\cdot \\ &\cdot \\ 0 &= q_L + q_{(L-1)}a_1 + \cdots q_{(L-N)}a_N \end{aligned} \quad [9]$$

Equation 9 can be represented in matrix form and partitioned into two parts. The lower partition is given by

$$\begin{Bmatrix} -q_{(M+1)} \\ -q_{(M+2)} \\ \cdot \\ \cdot \\ \cdot \\ -q_L \end{Bmatrix} = \begin{bmatrix} q_M & q_{(M-1)} & \cdot & \cdot & \cdot & q_{(M-N+1)} \\ q_{(M+1)} & q_M & \cdot & \cdot & \cdot & q_{(M-N+2)} \\ \cdot & & & & & \\ \cdot & & & & & \\ \cdot & & & & & \\ q_{(L-1)} & q_{(L-2)} & \cdot & \cdot & \cdot & q_{(L-N)} \end{bmatrix} \begin{Bmatrix} a_1 \\ a_2 \\ \cdot \\ \cdot \\ \cdot \\ a_N \end{Bmatrix} \quad [10]$$

For $M = N$, the resulting system of equations is underdetermined if $L < 2N$, and it is overdetermined if $L > 2N$. In both cases, the resulting matrix is not square. The rows of this matrix contain consecutive sections of the measurements of q_n obtained by a moving window containing $N - 1$ elements.

Once the coefficients a_i are determined from solving the equation system given by Eq. 10, the coefficients Z_k are obtained from

$$Z_k = roots(A(Z) = 1 + a_1 Z^{-1} + \cdots a_N Z^{-N}) \quad [11]$$

for $k = 1,2,\ldots N$. The resonant angular frequencies (ω_k) and damping ratios (ξ_k) are then computed using Eqs. 5 and 6, respectively. The coefficients $\tilde{A}_k$ are obtained by solving the system of equations defined by Eq. 3. These coefficients are complex number because of Z_k. Finally, the amplitude (A_k) and phase angle (θ_k) of each exponential function are computed from

$$A_k = |\tilde{A}_K| = \sqrt{(real(\tilde{A}_K))^2 + (imag(\tilde{A}_K))^2} \quad [12]$$

and

$$\theta_K = \tan^{-1}(\frac{imag(\tilde{A}_k)}{real(\tilde{A}_k)}) \quad [13]$$

The selection of the appropriate order (N) is one of the most critical aspects of any parametric method (Braun and Hammond 1986). There is no a single theory for the determination of the optimum order for the CEM. If a low model order is selected, the obtained frequency response function has insufficient resolution; on the other hand, a high model order can yield false peaks in the frequency response function. In this work, the order of the CEM is determined based on the residual sum of square errors between the original and fitted signals. The fitted signal is reconstructed using only the exponential functions identified as vibration modes.

3 TESTING METHODOLOGY

The proposed new technique is demonstrated by performing RC testing on a dry-sand specimen in free-vibration under loading (L) and unloading (U) conditions, two isotropic confinements (40 kPa and 100 kPa), and different shear strain levels (L1, γ_{max} = 1.34x10^{-5} up to L9, γ_{max} = 1.52x10^{-3}). In this work, the effects of the additional damping ratio introduced by the RC driving system or EMF damping (Cascante et al. 2003, 2005) are not removed from the time signals. The EMF damping is actually used to increase the real damping ratio of the sand specimen to show the validity of the new methodology when a wider range of damping ratios is present in a signal. Therefore, the free-decay damping ratios presented in the following sections are not the correct damping ratios for the dry-sand specimen. The correct damping ratios are computed using the transfer function method. The removal of EMF damping from free-decay tests has been addressed in previous studies (Cascante et al. 2003, 2005, Wang et al. 2003, Meng and Rix 2003).

The shear wave velocity and damping ratio are computed for each shear strain level applied to the specimen; which is given in terms of the height of the specimen (H) and the maximum displacement of the free-decay response (d)

$$\gamma_{max} = \frac{2d}{H} \quad [14]$$

The displacement time history is computed from integrating twice the acceleration time history measured on the driving plate at the top of the specimen. The shear wave velocity is computed from

$$V_s = \frac{\omega . H}{a} \quad [15]$$

where the coefficient a is obtained by solving the moment equilibrium equation for a cylindrical specimen under fixed-free boundary conditions; which is given by

$$\frac{I}{I_0} = a \tan(a) \quad [16]$$

The mass polar moment of inertia of the specimen I is computed from the specimen properties; whereas the corresponding moment of inertia of the driving plate I_0 is measured experimentally. The resonant frequency ω and damping ratio ξ are computed by curve-fitting the transfer function of the system (frequency domain analysis) and the free-decay responses (CEM, time domain analysis). For the calculation of the transfer function, the input signal is the force applied by the driving plate to the specimen, which is proportional to the current through the coils, and the output signal is the response of the accelerometer at the top of the specimen.

4 EXPERIMENTAL SETUP

Figure 1 presents a schematic diagram of the instrumentation used in this work. A square pulse is generated by a function generator (HP-33210A) to excite the driving coil system. The low-power input signal is amplified by a power amplifier (Bogen 250W). The axial deformation of the specimen is measured with an LVDT (Schaevitz 500HR) mounted inside the RC device. The free-decay of the specimen is measured with an accelerometer (PCB 353B65), which is mounted on the driving plate at the top of the specimen.

The cell and specimen pressures are controlled independently by a pneumatic pressure control panel (Brainard-Kilman E-400). The maximum pressure of the system is 685 kPa. The height and radius of the specimen are $H = 145$ mm and $R = 35$ mm, respectively.

The output signal of the accelerometer and the impulsive excitation (input signal) are processed with a dynamic signal analyzer (HP-35665A) to compute the transfer function. The resonant frequency and damping ratio are extracted from the measured transfer function. Finally, the measured free-decay response of the specimen is stored in a computer.

5 RESULTS, ANALYSIS, AND DISCUSSION

To demonstrate the proposed methodology, the evaluation of the damping ratio and shear wave velocity of a dry-sand specimen as function of the maximum shear strain are presented next. The results from the CEM under two isotropic confinements (41 kPa and 100 kPa) are compared with standard RC results (transfer function

and free vibration of a SDOF system) for different shear strain levels (L1 to L9).

5.1 Isotropic confinement $\sigma_0 = 41$ kPa

The free-decay response of the soil specimen is obtained for a wide range of shear strains. In this work, low strains are defined as $\gamma \leq 4 \times 10^{-5}$; medium strains as $4 \times 10^{-5} < \gamma \leq 4 \times 10^{-4}$; and large strains as $\gamma > 4 \times 10^{-4}$. In loading condition, four RC tests correspond to low strains (L1-L4); three RC tests, at medium strains (L5-L7); and two RC tests, at large strains (L8-L9). Furthermore, two RC tests at medium (U1-U2) and at low (U3-U4) strains were performed for unloading condition.

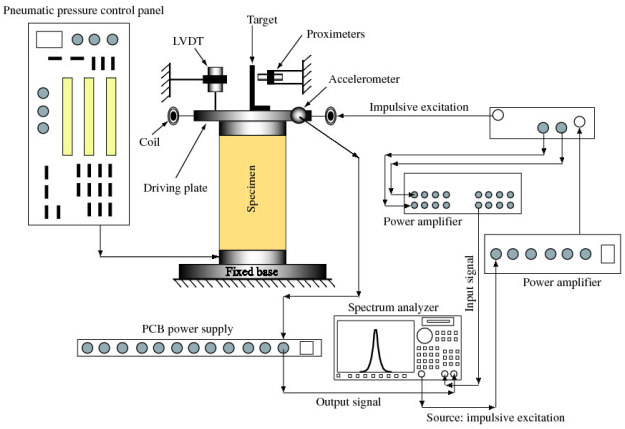

Figure 1. Schematic diagram of the instrumentation used for the free-decay response in RC testing

Figure 2 shows typical results indicating that the curve-fitting of a large strain free-decay response (test L8) using a SDOF model cannot predict correctly the measured signal. The ordinate axis represents the measured acceleration on the driving plate at the top of the specimen. The maximum shear strain applied to the soil specimen is $\gamma_{max} \approx 6.6 \times 10^{-4}$. The curve-fitted resonant frequency and damping ratio are $f = 45.0$ Hz and $\xi = 11.5\%$. The nonlinear behavior characterized by the decrease in the period (increase in frequency) as the acceleration amplitude decreases is observed in the last three cycles of the signal.

The curve-fitting of the large-strain test L8 using the CEM is presented in Figure 3b. The predicted response using four exponential functions is in agreement with the measured one for all the time window. The exponential functions identified using the CEM are shown in Figure 3a. The identified resonant frequencies and damping ratios are also shown in this figure. The lowest frequency identified using the CEM is called the main frequency of the system; whereas the other ones are referred as higher frequency components. The SDOF method overestimates the main frequency by 13% and underestimates the damping ratio by 60% with respect to the values obtained by the CEM.

The plots of the instantaneous frequency and damping ratio for the large-strain test L8 using the Hilbert transform are presented in Figure 4. The instantaneous damping ratio is maximum at time $t = 13.3$ ms ($\xi = 24\%$); which corresponds to an instantaneous frequency of $f = 42.3$ Hz ($f = \omega/2\pi$).

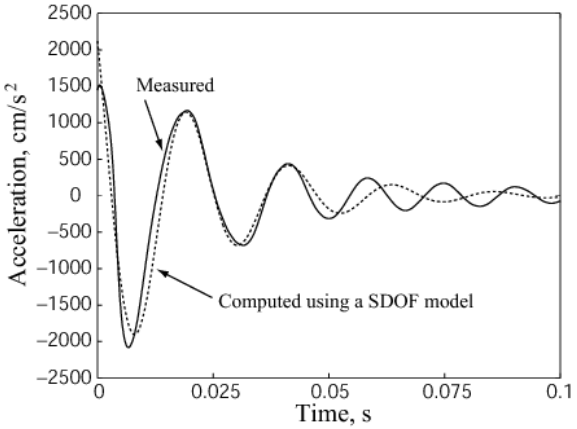

Figure 2. Measured free-decay response in a large strain RC testing (test L8) and curve-fitted signal using a SDOF model

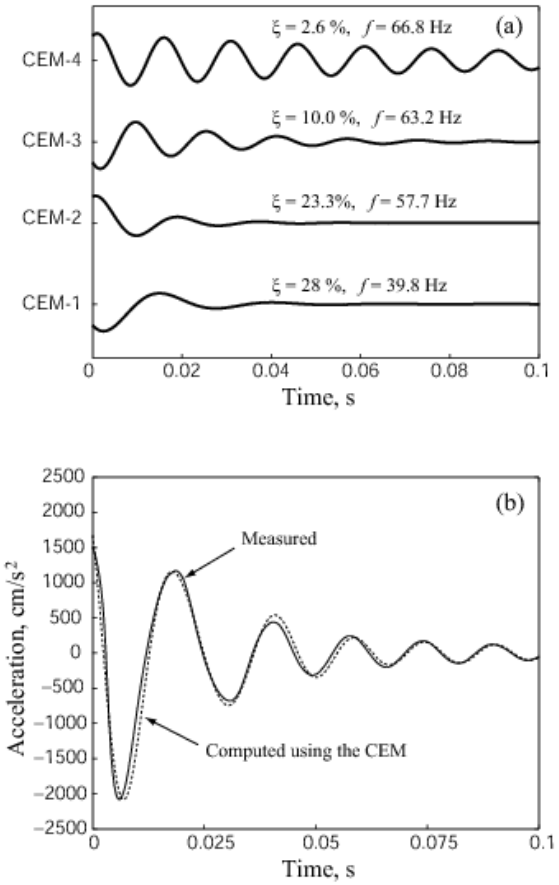

Figure 3. Decomposition of a large strain free-decay test (L8): Main four exponential functions from the CEM (a), measured and curve-fitted responses by superposing the main four exponential functions (b)

This damping ratio characterizes the attenuation of the first half a cycle of the signal (Figure 4a). The instantaneous frequency is 9% greater whereas the damping ratio is 14% smaller than the corresponding values obtained from the CEM for the main vibration mode. These differences are likely generated by the inability of the Hilbert transform to correctly predict the frequency and damping ratio at the starting point of the response ($t < 13.3\ ms$). In general, the instantaneous frequency increases and the damping ratio decreases as the shear strain level decreases (low accelerations). The maximum frequency and minimum damping ratio from the instantaneous plots tend toward the corresponding values obtained from the CEM.

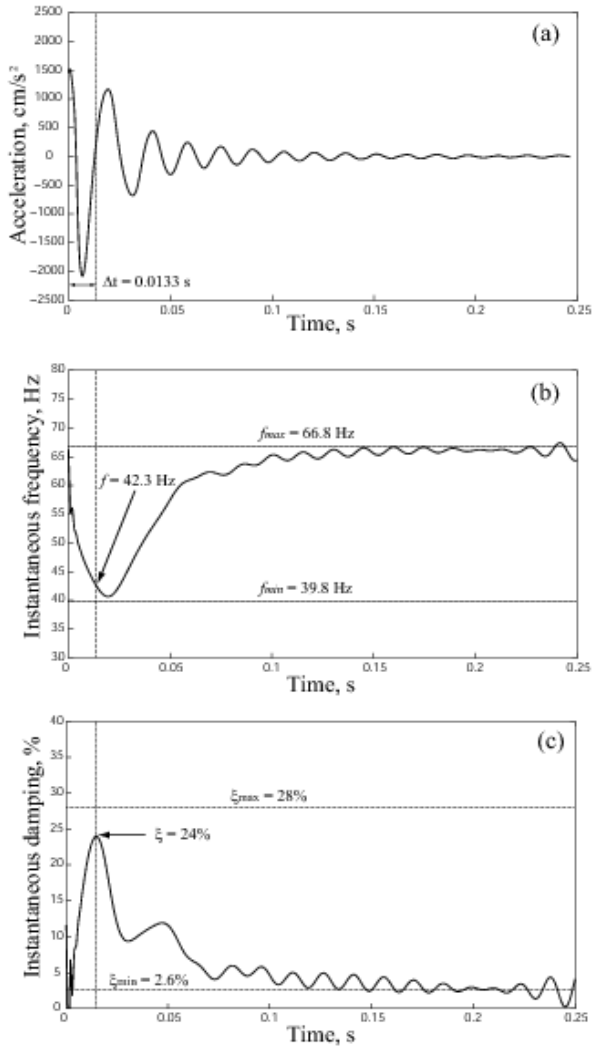

Figure 4. Use of the Hilbert transform on a large-strain free-decay test (L8): time history (a), instantaneous frequency (b), instantaneous damping (c)

The results from the CEM and the SDOF model are similar for small strains; the maximum differences are less than 9% and 1% for damping ratios and resonant frequencies, respectively. As expected, the resonant frequency decreases and the damping ratio increases with increasing shear strain levels (loading condition).

Two and three exponential functions are required to model the free-decay response at medium strain levels. Even though the main resonant frequencies estimated from the SDOF model and the CEM are similar (maximum difference less than 2%), the SDOF model underestimates the damping ratio by 21%, 31%, and 57% for shear strains of 0.65×10^{-4}, 1.4×10^{-4}, and 2.8×10^{-4}, respectively.

At higher strain levels, the free-decay response is modeled by four exponential functions. The maximum difference between the SDOF model and the CEM for the main resonant frequencies is 13%. On the other hand, the SDOF model underestimates the damping ratio in 59% and 38% for shear strains of 6.7×10^{-4} and 16.0×10^{-4}, respectively. For the test L9, $\gamma_{max} = 16.0 \times 10^{-4}$, two of the exponential functions have high damping ratios (40.6% and 23.2%). The higher value operates in the first half a cycle of the response. Damping ratios for dry sand between 20% and 25% and shear strains in the order of $\gamma_{max} = 20.0 \times 10^{-4}$ have been reported by other researchers (e.g. Zambelli et al. 2006). However, previous measurements are performed for at least one cycle of excitation. As indicated before, the damping ratios presented for the free-decay method are not corrected by EMF damping; this damping increases with decreasing resonant frequency and material damping (Cascante et al. 2003).

During the unloading phase, resonant frequencies increased and the damping ratios decreased according to the decrease in shear strain levels. Two and three exponential functions are required to model the free-decay response at medium shear strains. At the end of the loading phase, the dry-sand specimen is stiffer than at the beginning of testing because of the reduction in void radio and change in fabric during loading. The increase in stiffness is evidenced by the 24% increase in the main resonant frequency (tests U4 and L1) and the 7% decrease in the damping ratio

Figure 5(a) presents the magnitude of the Fourier spectra for all tests during loading. The nonlinear behavior (decrease in resonant frequency, increase in damping ratio) is clearly shown when the shear strain increases from $\gamma_{max} = 0.13 \times 10^{-4}$ to $\gamma_{max} = 16.0 \times 10^{-4}$.

For low strain levels (black solid curves), only one resonant peak is observed. A second resonant frequency is clearly observed in the L5 test. The resonant peak widens as the shear strain increases because of the increase in damping ratio. This effect is accentuated when the shear strain increases (tests L7-L9). When $\gamma_{max} > 7.0 \times 10^{-4}$, a well defined second resonant peak is observed at a frequency of 65 Hz.

The magnitude Fourier spectra for the unloading phase are shown in Figure 5(b). As expected, the resonant frequency increases and the damping ratio decreases when the maximum shear strain decreases. In general, the results from the magnitude Fourier spectra are in agreement with the dynamic characteristics obtained by the CEM.

The variation of damping ratio with the maximum shear strain during loading and unloading conditions is presented in Figure 6. The $\xi - \gamma_{max}$ curves obtained using the SDOF model (time domain) and the transfer function method (frequency domain) are similar for shear strains $\gamma_{max}>10^{-4}$; because the EMF effect is stronger at low strain levels. The CEM predicts higher damping ratios for the fundamental frequencies because it is able to evaluate the damping ratio in less than one cycle of the free-decay response. The difference between the CEM and the SDOF method increases from 9% to 59% as the shear strain level increases. The damping ratios from the CEM for the higher frequency components are closer to the correct values (transfer function results) because the EMF effects decrease with the increase in resonant frequency.

The reduction in damping ratio with frequency indicates that the CEM can be potentially used to study frequency effects in dynamic soil properties. This potential use is also indicated in Figure 7; which shows that the shear stiffness of the soils specimen increases with frequency as reported in previous studies (Khan et al. 2008, 2010, Zambelli, et al.2006).

Figure 7(a) shows the degradation curves for the shear wave velocity. In general, the degradation curves from the transfer function and free vibration methods are similar (maximum difference of 15%) for shear wave velocities computed for the main frequencies because the effect of the EMF damping on wave velocities is not significant. Shear wave velocities computed for high frequency components at low shear strains follow the degradation trend of the main frequency component. However, the high frequency components at medium shears trains (tests L5, L6, and L7) show greater shear wave velocities. This behavior is in agreement with previous observations showing that the sand specimen becomes stiffer after the application of high strain level excitations.

The $\mathbf{V_s - \gamma_{max}}$ curves for unloading condition are presented in Figure 7(b); which includes the higher frequency components at low and medium strain levels, for loading and unloading conditions. Shear wave velocities for the main and high frequency components (including loading condition) show a similar degradation patterns. The shear wave velocities from the CEM are in general higher than the transfer function results; this effect may be related to frequency or number of cycles effects and requires further investigation. The unloading shear wave velocities increased up to 20% with respect to the loading condition.

5.2 Isotropic confinement $\sigma_0 = 100$ kPa

The results for a confinement of 100 kPa are presented only for the loading condition because the results from the unloading condition are similar to the results presented for the confinement of 41 kPa. A total of nine free-vibration and transfer function tests are performed for shear strain levels between γ_{max} = 6.6x10^{-6} and γ_{max} = 6.0x10^{-4}. The magnitude spectra for all tests are shown in Figure 8. At low strains, the resonant frequency increases by a factor of 1.27 when the confinement is increased from 41 kPa to 100 kPa; this increase corresponds to an exponent b=0.27 for the velocity-confinement relationship ($V_s = a\sigma^b$); which is typical for the tested sand (Cascante and Santamarina 1996).

The damping ratio as function of the maximum shear strain is presented in Figure 9(a). The decrease in damping at low-strain levels with confinement is also typical for the tested sand. As indicated before, the damping ratios for the high frequency components are smaller than the corresponding values for the main frequency component because of the EMF effect. As the EMF damping decreases with an increase damping ratio, the difference between the CEM and the transfer function results decreases. The damping ratio obtained from the SDOF model is 12% smaller than the corresponding value estimated from the CEM for $\gamma_{\max} \approx 6.0 \times 10^{-6}$, increasing up to 80% at large strains ($\gamma_{\max} \approx 3.5 \times 10^{-4}$).

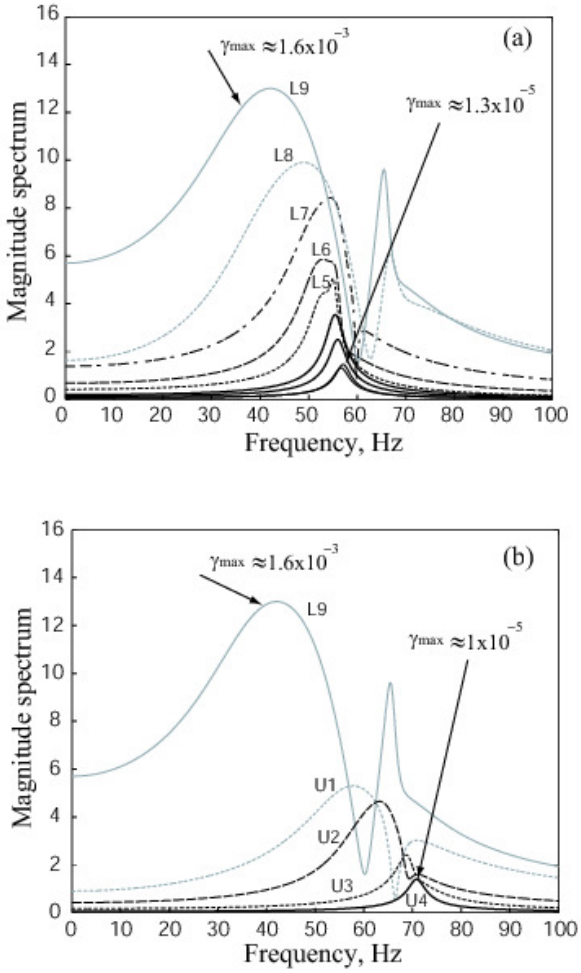

Figure 1. Magnitude spectra for loading (a) and unloading (b) RC tests

The degradation curve of shear wave velocity is presented in Figure 9(b). The maximum difference between the shear wave velocities from the transfer function and free vibration methods as well as the CEM is less than 2% for $\gamma_{max} \approx 1.0 \times 10^{-5}$, and 10% for $\gamma_{max} \approx$

3.6×10^{-4}. As expected, because the EMF effects in the resonant frequency are small and the fabric of the specimen is less perturbed at higher confining pressures. Small fabric changes are also confirmed by the agreement between the shear wave velocities of high and main frequency components.

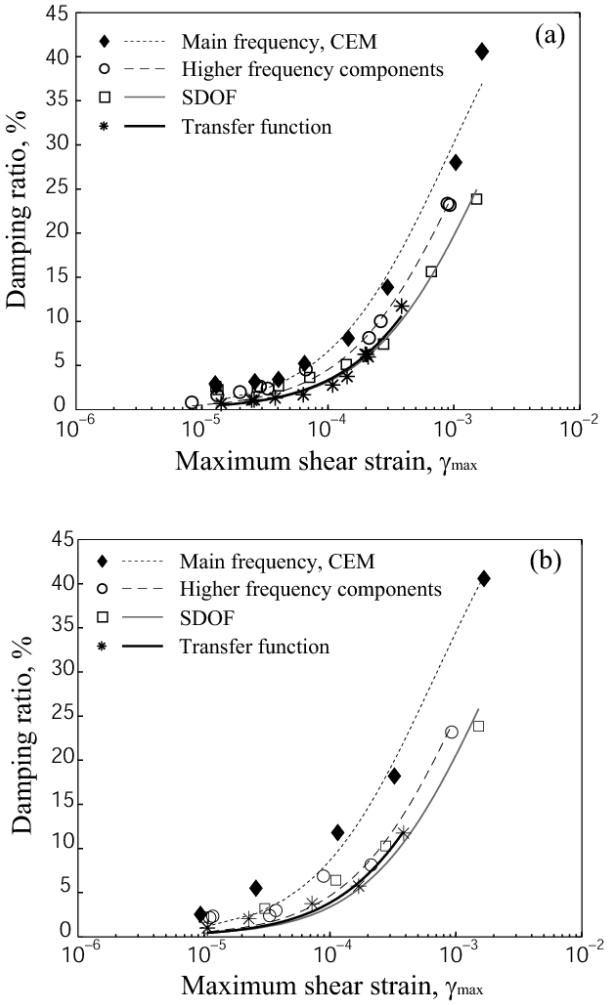

Figure 2. Damping ratio against maximum shear strain for loading (a) and unloading (b) conditions

6 CONCLUSIONS

This paper presents a new methodology for the dynamic characterization of soils using the free-decay response in RC testing. The new methodology is based on representing the free-decay response as a combination of damped exponential functions (complex exponential method, CEM). The use of the CEM is demonstrated on a dry-sand specimen with artificially increased damping (EMF damping) to cover a wider range of damping ratios with one specimen. The CEM is used to measure resonant frequencies and damping ratios of the dry-sand specimen at different shear strain levels (γ_{max} = 6.6 x10^{-6} up to γ_{max} = 1.52x10^{-3}).

The experimental results show that the damping ratio is underestimated up to 80% at large shear strain levels when the traditional SDOF model is used. The CEM can be used to measure high damping ratios for the fundamental frequencies because it is able to evaluate the damping ratio in less than one cycle of the free-decay response; unlike the standard SDOF model.

The new methodology can be successfully used to measure the degradation curves of shear wave velocity and damping ratio using free-decay tests; which minimize the number of cycles imposed on the specimen and thus the disturbance of the initial conditions of the specimen during testing. The specimen disturbance introduced during large-strain RC testing using the transfer function method is evidenced by the increase in shear wave velocity and the decrease of damping ratio, especially at low confinements.

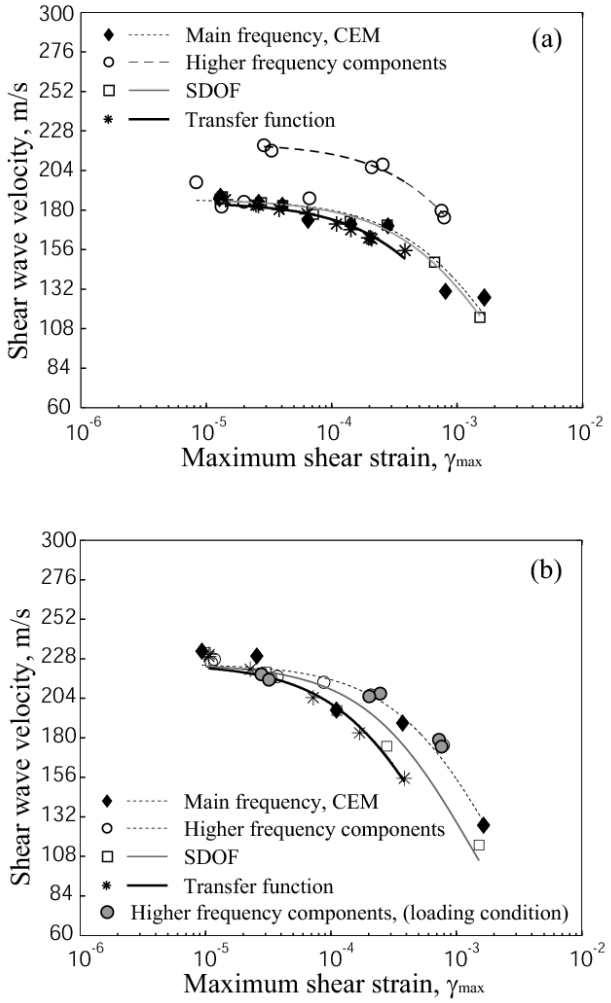

Figure 3. Shear wave velocity against maximum shear strain for loading (a) and unloading (b) conditions

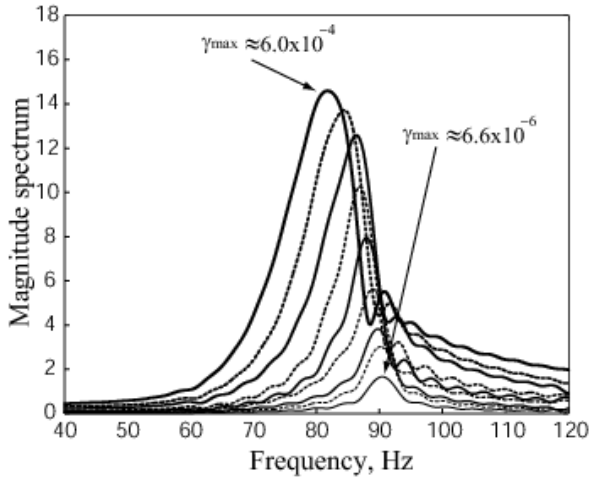

Figure 8. Fourier magnitude spectra for loading

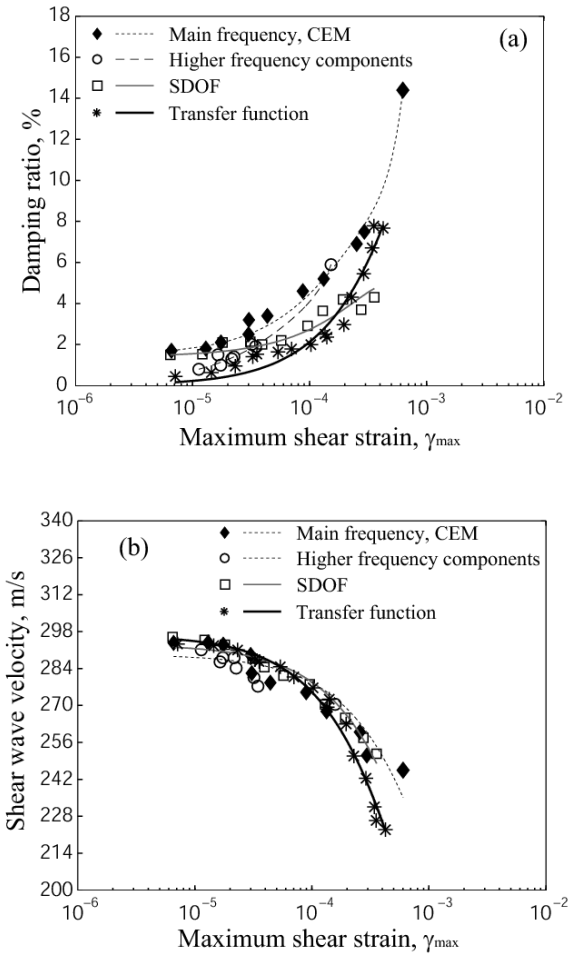

Figure 9. (a) Damping ratio and (b) shear wave velocity against maximum shear strain

7 ACKNOWLEDGMENTS

The authors would like express their gratitude to the Natural Sciences and Engineering Research Council of Canada (NSERC), University Network of Excellence in Nuclear Engineering (UNENE), and Hydro-One for the funding provided for this research.

7.1 REFERENCES

Braun, S. and Hammond, K. J. 1986.Parametric methods.Academic Press. Editor Braun, S., Chapter 5, pp. 103-138.

Cascante, G., Vanderkooy J., and Chung, W., 2003.Difference between current and voltage measurements in resonant-column testing. Canadian Geotechnical Journal 40(4): 806-820.

Cascante, G., Vanderkooy, J., and Chung, W., 2005.A new mathematical model for resonant-column measurements including eddy-current effects. Canadian Geotechnical Journal, 42(1): 121-135.

Cascante, G., and Santamarina J. 1996. Interparticle Contact Behaviour on Wave Propagation." Journal of Geotechnical Engineering, ASCE, Vol. 122, No. 10, 831-839.

Hardin, B. O. and Richart, F. E., Jr., 1963, Elastic wave velocities in granular soil, Journal of the Soil Mechanics and Foundations Division, ASCE, Vol. 89, No. SM1, pp. 33–63.

Khan, Z., Cascante, G., and El-Naggar, H., Lai, C.G., 2008. Measurement of Frequency Dependent Dynamic Properties of Soils Using the Resonant Column Device.Journal of Geotechnical and Geo-environmental Engineering, ASCE, 134(9), 1319-1326.

Khan, Z., Cascante, G., and El-Naggar, H., 2010. Frequency dependent dynamic properties of soils from resonant column and cyclic triaxial tests.Journal of the Franklin Institute.(In press).

Meng, J., and Rix, G.J. 2003.Reduction of equipment-generated damping in resonant column measurements, Géotechnique. 53(5), 503-512.

Osborne, M. R. and Smyth, G. K. 1995. A modified Pronyalgorithm for fitting sums of exponential functions. SIAM Journal of Scientific Computing, Vol. 16, pp. 119-138.

Santamarina J.C. and Cascante, G. 1996. Stress anisotropy and wave propagation. a micromechanical view. Canadian Geotechnical Journal, 33(5): 770-782.

Wang, Y.H., Cascante, G., and Santamarina, J.C. 2003. Resonant column testing: the inherent counter emf effect. Geotechnical Testing Journal, ASTM, 26(3): 342-352.

Wilson, S. D. and Dietrich, R. J., 1960, “Effect of consolidation pressure on elastic andstrength properties of clay,” Proceedings, ASCE Soil Mechanics and FoundationDivision, Research Conference on Shear Strength of Cohesive Soils, Boulder,CO, ASCE, New York.

Zambelli, C., di Prisco, C., d’Onofrio, A., Visone, C. and de Magistris, F. 2006. “Dependency of the mechanical behaviour of granular soils on loading frequency: experimental results and constitutive modeling,” Geotechnical Symposium in Roma, March 16-17.